

## Article

# Thermal and Moisture Management in the Microclimate of Socks for Diabetic Foot Care: The Role of Mohair-Wool Content

Adine Gericke<sup>1</sup>  and Mohanapriya Venkataraman<sup>2,\*</sup> 

<sup>1</sup> Department of Chemistry and Polymer Science, University of Stellenbosch, Stellenbosch 7600, South Africa; agericke@sun.ac.za

<sup>2</sup> Department of Material Engineering, Faculty of Textile Engineering, Technical University of Liberec, 461 17 Liberec, Czech Republic

\* Correspondence: mohanapriya.venkataraman@tul.cz

**Abstract:** In diabetic patients, optimised plantar health necessitates meticulously designed hosiery. These specialised socks facilitate a healthy microclimate at the skin–textile interface. This requires that stable conditions of temperature and humidity are maintained during wear. This study investigated the thermal resistance and moisture management properties of socks for diabetics. Fabrics and socks were evaluated on the Alambeta and thermal foot manikin instruments and in wear trials. A novel in vitro method, mimicking in-use conditions, was employed to validate findings and assess sock performance during wear. Fabric structure, especially thickness, had a greater impact on thermal resistance than fibre composition, suggesting that socks with different levels of thermal resistance can be customised according to individual preferences. In terms of moisture management, mohair–wool socks outperformed polyester socks, maintaining significantly lower humidity between the skin and the sock, and meeting the requirement to prevent the drying out of the microclimate significantly better. The enhanced moisture vapour sorption exhibited by the mohair–wool fabric contributes to this effect. Overall, the findings suggest that mohair–wool is an excellent fibre choice for diabetic socks, due to its unique moisture management properties and the possibility to tailor thermal properties through fabric structural design.

**Keywords:** thermo-physiological comfort; microclimate; thermal resistance; moisture management; mohair; wool; bamboo viscose; recycled polyester



**Citation:** Gericke, A.; Venkataraman, M. Thermal and Moisture Management in the Microclimate of Socks for Diabetic Foot Care: The Role of Mohair-Wool Content. *Fibers* **2024**, *12*, 53. <https://doi.org/10.3390/fib12070053>

Academic Editor: Martin J. D. Clift

Received: 17 April 2024

Revised: 1 June 2024

Accepted: 13 June 2024

Published: 25 June 2024



**Copyright:** © 2024 by the authors. Licensee MDPI, Basel, Switzerland. This article is an open access article distributed under the terms and conditions of the Creative Commons Attribution (CC BY) license (<https://creativecommons.org/licenses/by/4.0/>).

## 1. Introduction

Mohair fibres, derived from the hair of the Angora goat, possess exceptional qualities that have made them highly sought after for luxury items such as scarves, jerseys, upholstery, carpets, and blankets. Their superior thermal resistance has been a key factor in their success. Recent industrial research and development efforts have focused on expanding the application of mohair and wool fibres to more functional products, including specialised socks for diabetic patients. Despite the remarkable success of these socks, limited research has been published on their performance properties [1,2].

Diabetes, a global pandemic, is estimated to cause a limb loss every 30 s worldwide [1,2]. “Diabetic foot”, characterised by the classic diabetic foot ulcer, is a consequence of long-term chronic diabetic complications affecting the lower limbs [3]. A seemingly minor skin laceration or crack can trigger a progression from a non-ulcerated condition of a foot at risk to an acute foot ulcer, potentially leading to amputation. Risk factors include any condition that can cause a small wound, from abrasion by ill-fitting footwear to untreated calluses or excessive skin dryness. Additionally, microbial growth and fungal infections must be prevented [3,4].

The use of special socks can be one way to reduce the incidence of foot ulcers in diabetic patients. Beyond providing a cushioning effect to protect the skin from injury, the primary requirement for diabetic socks is to create a stable microclimate between

the skin and the sock, even under varying external environments and physical activity levels [5]. This will prevent the build-up of moisture that can cause discomfort and create an ideal environment for microbial growth. Another critical requirement is to prevent the microclimate from becoming too dry, as this can lead to skin cracking and lacerations that may become infected [6].

Maintaining a stable microclimate between the skin and surrounding textiles depends on the textile's thermo-physiological properties. The main parameters for the objective evaluation of thermo-physiological comfort properties in socks are heat transfer resistance (thermal resistance) and moisture management [7,8]. The skin continuously produces moisture in the form of insensible perspiration, resulting in the accumulation of moisture vapour in the microclimate. Dissipation of moisture vapour from the microclimate to the environment, facilitated by a concentration gradient, occurs through the interstitial spaces in the textile fabric, a process that is usually sufficient in knitted fabrics. Increased physical activity or skin temperature can lead to sensible perspiration, introducing liquid water onto the skin surface. In this case, either the liquid water must evaporate and dissipate from the microclimate as moisture vapour (as described above) or be absorbed by the textile covering the skin. The effective dissipation of absorbed water relies on the textile structure's ability to wick moisture from the wet area to the dryer environment without being absorbed by the fibres. If water is absorbed into the fibre structures, the wicking process is hindered, causing the socks to become wet and uncomfortable [9,10].

In the case of socks, the situation becomes more complex when shoes, which can be made from various materials with differing moisture and air transmission properties, are worn over the socks. This factor must also be considered when selecting test methods for evaluating sock fabrics.

Liquid moisture transmission in synthetic fibre materials is generally better than in materials consisting of natural fibres. Polyester fibres have a very low moisture regain, which implies that the fibres absorb very little water. Textile structures made of polyester, however, allow moisture to move into the interstitial spaces between fibres and yarns. Normally polyester fibres and fabrics do not retain water and imbibed water is readily released, which gives the material its quick-drying properties [11,12]. If this process is interrupted, as in the typical situation where the socks are covered by a type of footwear material; moisture vapour will not be allowed to escape to the environment, causing liquid moisture to accumulate either between the sock and the shoe or against the skin inside the sock.

Mohair and wool fibres are known for their excellent moisture management properties. Wool is often referred to as nature's own smart fibre. This is due to its unique combination of performance properties that relies mostly on its hygroscopic nature, meaning the fibres can absorb large amounts of moisture (in liquid or vapour form) without feeling wet. This property is crucial for regulating moisture between the skin and the sock. Hygroscopic fibres absorb moisture, preventing buildup in this microclimate. This lowers humidity, creating an environment less favourable for microbial growth. The hygroscopic fibres have the ability to retain moisture and have a slow rate of evaporation, allowing the moisture vapour gradient between the skin and the external environment to be kept at a minimum and lowering the rate of loss of body moisture [11]. This minimises moisture loss from the body while still allowing socks to release moisture back into the microclimate when it becomes dry. It is postulated that this self-regulating mechanism creates a stable and comfortable microclimate inside the sock.

The thermal resistance of fibres depends on their ability to conduct heat and heat loss through a textile structure and relates mainly to the thermal conductivity of the fibrous matter, the thickness of the fabric, and its porosity [13–15]. The thermal conductivity of regenerated cellulose fibres ( $0.289 \text{ W K}^{-1} \text{ m}^{-1}$ ) and polyester ( $0.272 \text{ W K}^{-1} \text{ m}^{-1}$ ) is significantly higher than that of wool and mohair ( $0.192 \text{ W K}^{-1} \text{ m}^{-1}$ ) [16,17]. Still air, however, has a thermal conductivity of  $0.024 \text{ W K}^{-1} \text{ m}^{-1}$  at  $0 \text{ }^\circ\text{C}$ , which is less than 10 times that of the average textile fibre. This can cause entrapped air within a textile

structure to have an overbearing effect on specific fibre properties. For this reason, it has been found that the thermal resistance of a fabric depends mostly on the fabric thickness and to a lesser extent on fibre content [2,16]. In the case of fabrics containing mohair, their high  $R_t$  is attributed to the three-dimensional crimp of the fibres that results in yarns and fabrics with many “open” spaces where motionless air can be trapped. Up to two-thirds of the volume in a piece of wool fabric can be occupied by air spaces. These air spaces are kept intact by the wool fibres’ resiliency and crimp [2].

The purpose of this study was to investigate the effect of the fibre content of diabetic socks on the complicated matter of maintaining the required moisture and temperature-related conditions in the microclimate in socks. To achieve this, different known test instruments and test methods were used to evaluate the thermal and moisture management properties of the socks. Socks were tested on the thermal foot manikin and in wear trials and fabric specimens (cut from the socks) were evaluated on the Alambeta and Permetest instruments to determine which could reliably describe how the socks perform during wear. This led to the development of a novel test method in which the moisture sorption properties of the individual fabrics as well as their effect on the conditions in the microclimate can be measured.

## 2. Methodology

For this study, three commercial sock samples were compared. The socks were all designed according to diabetic footwear requirements. Variance in fibre content was achieved by using three different main yarn types during the knitting process. These included firstly a yarn spun of predominantly mohair and wool fibres (MW), in which equal amounts of mohair and wool fibres were blended with a small amount of nylon staple fibres to improve the spinnability and tensile strength. The MW yarn was used in two of the sock samples. The other two yarns were spun from bamboo viscose staple fibres (BV) and recycled polyester staple fibres (PETR). During the knitting of all the socks, a low amount of nylon-elastane-covered filament yarn (NE) was added to provide elasticity.

The yarns were analysed regarding fibre composition and size and are described in Table 1. Scanning electron microscope (SEM) images were obtained to closely examine the physical structural characteristics of the fibres and yarns that could affect or explain the results.

**Table 1.** Description of yarns used to knit socks.

Yarn Ref.	Yarn Description					Portion	Yarn Size
	Mohair	Wool	Nylon	Bamboo Viscose	Recycled PET		
MW	40	40	20			>90%	40 Tex
BV				100		>90%	36 Tex
PETR					100	>90%	33 Tex
NE						<10%	27.8 Tex

The three socks were referenced as S-MW, S-PETR, and S-MWV and are depicted in Figure 1. S-MW and S-PETR were knitted with, respectively, MW and PETR yarns. In the third sock, S-MWV, areas knitted with the MW yarn were strategically alternated with areas knitted with BV yarn, as illustrated in Figure 1, to produce a sock comprising 30% MW- and 70% BV-containing areas (over total sock surface area). The purpose of this design was to increase the thermal conductivity on the upper foot and ankle areas (by using BV) to decrease the thermal resistance of the total sock, and consequently, prevent overheating of the foot. The positioning of the MW yarn around the areas on the foot that are critical for diabetic foot care ensures that thermal and moisture management properties similar to those in the S-MW sock can be expected here. In all cases, a 3 cm ribbed edging around

the top part of the leg ensures that the sock fits snugly around the leg, without exerting pressure on the leg.

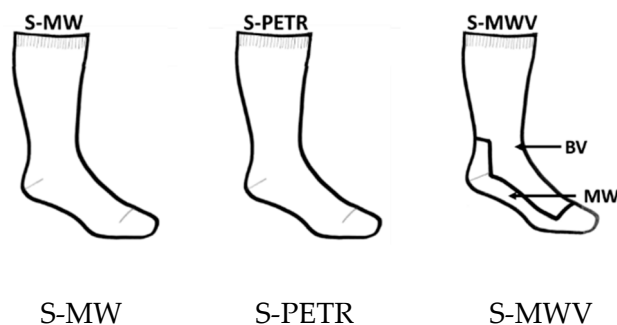


Figure 1. Designs for socks referenced S-MW, S-PETR, and S-MWV.

All the socks were knitted on automatic 95-needle sock knitting machines with a cylinder diameter of 4 inches in a basic pile knit structure (commonly used in socks). During the knitting process, a small percentage of nylon-elastane-covered filament yarn (NE) (<10%) was added with an extra feeder to provide elasticity. The knitted fabric structures of the socks were analysed, and the structural details are technically described in Table 2. The average weight of the sock fabrics (g/m<sup>2</sup>) was determined by weighing 100 cm<sup>2</sup> cuttings of fabric with a circular cutter to ensure accuracy. Fabric thickness (mm) was measured on the Alambeta. Fabric porosity was calculated as defined in Equation (1) [18].

$$P = 1 - \frac{m}{p \times h} \tag{1}$$

with P the relative porosity (%), m the fabric weight (g/m<sup>2</sup>), p the fibre density (g/m<sup>3</sup>), and h the fabric thickness (mm).

Table 2. Technical description and graphical depiction of knitted structures of socks.

Sock Ref.	Weight (g/m <sup>2</sup> )	Thickness (Average) (mm)	Sock Fabric Analyses		
			Porosity (%)	Stitch Density, Wales/Courses	Pile Knit Structure
S-MW	615	4.2	88.8%	5.5/6	
S-PETR	668	4.6	88.9%	5.5/6	
S-MWV	588	4.4	89.5%	5.5/6	

Samples were conditioned for 24 h in standard atmospheric conditions (65% RH and 20 °C) before weighing and weighed under the same conditions according to ISO 139:2005 and ISO 3801:1977.

The main parameters for the objective evaluation of thermo-physiological comfort properties in textiles are heat transfer resistance (thermal resistance) and moisture management [7,8]. In this study, the main aim was to comprehensively evaluate the performance of three sets of socks under varying conditions. Different methods and instruments were employed to compare their performance properties and assess the reliability of these measurements in predicting suitably for this specific end-use. The thermal resistance (Rt) and moisture vapour permeability (MVP) of the fabrics were evaluated on the Alambeta and Permetest instruments. To test the Rt of the socks during wear, further tests were performed on the thermal foot manikin (TFM). Further evaluation of the conditions in the microclimate during wear included wear trials, where the temperature and moisture conditions in the

microclimate inside the sock during wear were logged with thermocron iButtons. A novel test method was furthermore developed to measure conditions in the microclimate in vitro to address limitations identified in previous tests.

The Alambeta instrument measures thermal comfort properties such as thermal resistance, thermal conductivity, thermal absorptivity, and fabric thickness on fabric samples. The instrument was developed by the Sensora Company from Czech Republic. During the test, the mounted sample is kept between hot and cold plates according to ISO11092. As soon as the hot plate comes into contact with the fabric sample (at a pressure of 200 Pa), the amount of airflow from the hot to the cold surface through the fabric is measured by heat flux sensors [19,20]. For this study, the  $R_t$ , as well as thickness ( $h$ ) of fabric specimens cut from the sock samples, were measured. The instrument and its operational details are shown in Figure 2. The measuring system of the Alambeta instrument is illustrated and the relevant parts of the instrument are indicated by the numbers 1 to 6. The sample to be measured (5) is mounted on the instrument base (6). A special heat-power-sensing block (4) is attached to a metal block (2) which maintains a constant temperature of 32 °C (which is higher than the sample temperature of 22 °C). When the measurement starts, the measuring head (1) containing the sensing block (2) drops down and touches the measured sample under a pressure of 200 Pa. This causes the surface temperature of the sample to suddenly change and the instrument computer then registers the transient temperature field in the thin slab of the sensing block. The instrument measures thermal conductivity  $\lambda$ , thermal resistance  $R$ , sample thickness, and the warm-cool feeling parameter (not discussed in this paper) and lasts less than 5 min.

Thermal resistance is inversely proportional to thermal conductivity and can be calculated by Equation (2):

$$Rt = \frac{h}{\lambda} \quad (2)$$

with  $Rt$  ( $K \cdot m^2 \cdot W^{-1}$ ) the thermal resistance,  $h$  (mm) the fabric thickness, and  $\lambda$  ( $W \cdot m^{-1} \cdot K^{-1}$ ) the thermal conductivity [21]. The results are reported as  $mK \cdot m^2 \cdot W^{-1}$  [14,19,22].

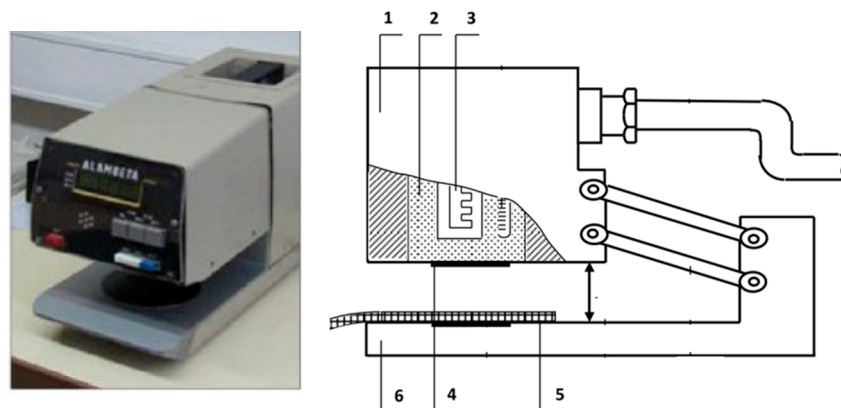


**Figure 2.** The Alambeta instrument and its operational details [23].

The water vapour permeability of fabric specimens was measured on the Permetest instrument, a fast-response measuring instrument for the non-destructive determination of the water vapour permeability (%). An image of the Permetest instrument and illustration of its working principle is shown in Figure 3. The results of the measurement are expressed in units defined in the ISO Standard 11092. To evaluate the water vapour permeability of a fabric, the test specimen is mounted over a slightly curved porous moistened surface (diameter about 80 mm) and exposed in a wind channel to parallel air flow of adjustable velocity. The measuring head is covered with a semi-permeable membrane to keep the measured specimen dry. At the start of the test, the heat flow value over the measuring head without a sample is registered. The test specimen is then inserted between the head and the orifice in the bottom of the channel. The specimen does not need to be cut to a

smaller size for testing and multiple layers of fabric can be tested. The instrument measures the amount of evaporation heat taken away from the active porous surface by a special integrated system and produces results within several minutes [24].

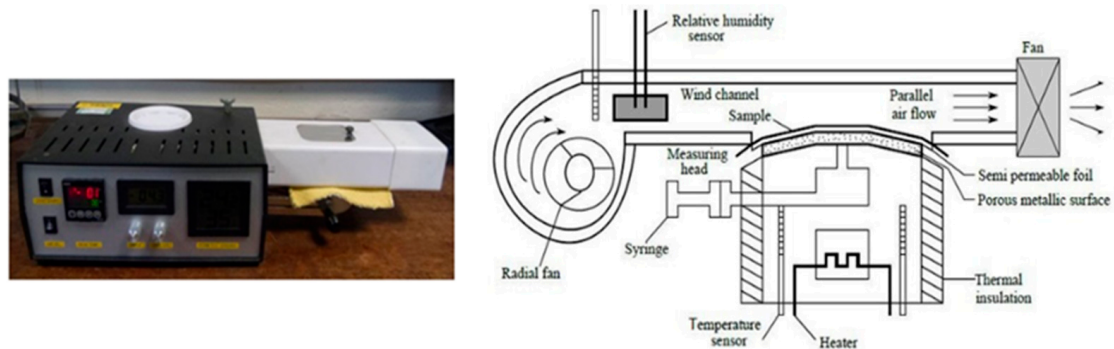


**Figure 3.** Image and explanation of the working principle of the Permetest instrument [24,25].

For this study, the water vapour permeability of the three sock structures was tested to confirm that it was comparable. The results indicated that all the fabric specimens cut from the socks had a water vapour permeability within the range of 21.5% to 25%. To resemble the cover layers that would be applicable when shoes are worn over the socks, two knitted fabric structures (CP1 and CP2), both made of polyester but of differing intensity, were selected. The MVP of CP1 was 62.7%, resembling that typically found in sports or leisure shoes, and CP2 had a low MVP of 8.6%, to resemble that found in formal shoes. The instrument is shown in Figure 3.

The thermal foot manikin is designed to measure the thermal resistance of a sock covering the foot and bottom leg area. It is divided into 13 segments, which are each separately heated to 35 °C. The segments can be individually controlled if required. A picture of the TFM cabinet as well as the thermal foot (indicating the divisions) is shown in Figure 4. To test the  $R_t$  of the sock, the sock specimen is fitted on the “foot”, covering the whole measuring surface, i.e., all the segments.

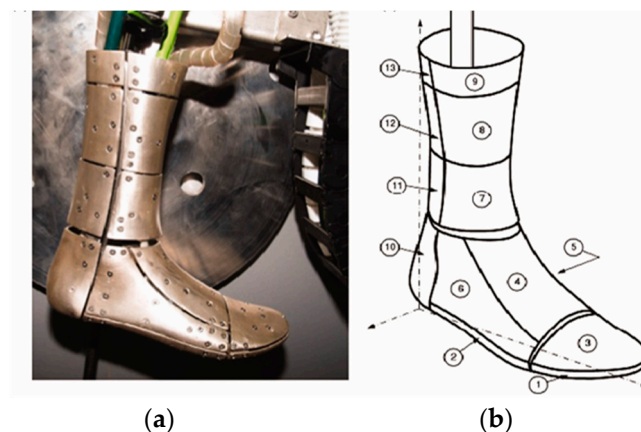


**Figure 4.** Pictures of (a) the TFM cabinet and (b) its mechanical leg, divided into 13 units [26].

Due to the occurrence of a certain amount of extension of the sock when fitted onto the thermal foot manikin, it is necessary to control the extension in different areas to prevent variations in thickness. In this study, two additional markings, M1 and M2 (measuring 10 and 15 cm), were added to the standard markings, to ensure that a consistent fit was achieved during the tests (Figure 5). During the placement of the sock on the manikin, the fit was adjusted to keep M1 and M2 constant to prevent elongation in the length of the sock (wale direction) and allow only the necessary elongation in the width (across wale) direction (across LC and FC).

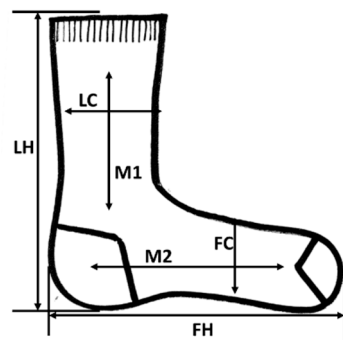


**Figure 5.** Illustration of how sock size measurements were taken. M1 and M2 indicate the extra markings that were used to ensure a consistent fit of the sock on the TFM during testing [7].

As required by the TFM procedure, critical sock dimensions such as the height of the sock leg (LH), the sock foot length (FL), half of the leg circumference (LC), and half of the foot circumference (FC) were measured to ensure that the three samples were comparable and to control the fit on the TGM. The total sock weights were also compared. After weighing, the socks were straightened out on a flat surface (as illustrated in Figure 5) and measured with a reading accuracy of 1 mm, as recommended by Rogina-Car et al. [7,8]. The sock dimensions are summarised in Table 3.

**Table 3.** Summary of the sock size dimensions measured as illustrated in Figure 5 before testing on the TFM.

Sock Reference	Sock Dimensions (cm)				Sock Weight (g)
	LH	FL	LC	FC	
S-MW	28	24	9.5	9.3	52.6
S-MWV	27	22.5	7.8	8.6	57.3
S-PETR	24	22.5	8.5	8.2	53.3

To measure the thermal resistance ( $R_t$ ) of a sock using the thermal foot model (TFM), a basic sock is carefully placed over the metal foot of the TFM and allowed to stabilise for 20–30 min in a controlled atmosphere with an ambient temperature of  $20 \pm 2$  °C and a relative humidity of  $65 \pm 5\%$ . The sock to be tested is then carefully fitted over the basic sock, ensuring that there are no wrinkles or gaps. The stabilisation period is then repeated. The thermal resistance of the sock ( $R_{tu}$ ) is then measured and recorded. This procedure is repeated for each sock sample. The thermal resistance of the tested sock is calculated by subtracting the thermal resistance of the basic sock ( $R_{t0}$ ) from the thermal resistance of the sock being tested ( $R_{tu}$ ) according to Equation (3).

$$R_t = (R_{tu} - R_{t0}) \quad (3)$$

The TFM used in this study was limited to measuring  $R_t$  under dry conditions, necessitating further trials with iButtons to investigate the microclimate conditions in vivo in the form of wear trials, during which the temperature and relative humidity within the microclimate inside the socks were monitored with small, standalone thermochrom data loggers known as iButtons. These iButtons were carefully secured on the skin inside the sock to record data at 60 s intervals [27]. The buttons were secured with adhesive tape to prevent movement inside the sock. A small piece of mesh fabric was secured between the iButton and the tape to ensure minimum contact between the sensor and the sock fabric. To simulate working or leisure conditions in an office or home setting, the participant was instructed to remain sedentary for most of the first 40 min, moving around every 10 min to maintain normal blood flow in the legs and feet. This was followed by 20 min of slow pedalling on a stationary cycle without significant exertion. Leather shoes were worn over the socks throughout the trials. To minimise metabolic variations and enhance accuracy,

only one participant was involved, and the procedure was repeated at least five times under ambient conditions of 65% RH and 20 and 24 °C. The iButtons are shown in Figure 6.

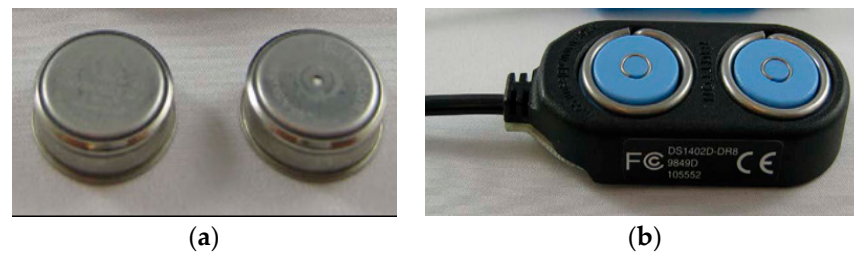


**Figure 6.** (a) ThermoChron iButton used to log temperature and humidity in the microclimate during wear trials and (b) the adapter [27].

A potential concern was the reliability of the measurement data obtained during wear trials due to the confined microclimate within which the iButtons operated. This raised the question of whether the conditions of this unique microclimate inside a sock could be replicated in a novel laboratory setup, inspired by the established upright cup method for evaluating moisture vapour permeability.

The laboratory setup for the customised covered jar (CJ) method comprised at least four small glass jars, each containing a fixed amount of water, over which a conditioned specimen was mounted securely. The temperature of the water inside the jar was kept constant by placing it in a temperature-regulated water bath and the laboratory ambient conditions were controlled. The method consists of two parts.

In part 1, the average weight change in the specimens after 60 min provided data on the percentage moisture sorption in the fabric. Note that for this test the term “% moisture sorption” refers specifically to the ability of the fibres in the specimen to absorb moisture vapour from the air. This differentiates the test from others that measure the ability of a fabric structure or fibres to absorb liquid moisture [10,18]. Resultantly, the results of this test reflect differences in moisture sorption of fabrics (under the condition that the water vapour permeability of the fabrics is comparable).

For the test procedure glass jars with a diameter of 55 mm were used. The jars have screw-on lids that mount samples tightly over a standardised central opening. This allows secure mounting of specimens in either single or multiple layers. The only way for evaporated water inside the jar to escape to the environment is through the specimen(s). Test parameters like the air gap underneath the specimen, water temperature, ambient temperature, and time of exposure were carefully controlled. To establish a standardised air gap of 40 mm between the sample and the water surface, the same volume of water was used in all the jars. The water bath was used to keep the water inside the jars at a constant temperature of 34 °C. The ambient conditions in the laboratory were  $20 \pm 2$  °C and 60–65% relative humidity. To determine the sorption, specimens were weighed before and after a 60 min running time to record  $W_0$  and  $W_{60}$ . The laboratory setup is illustrated in Figure 7a. The % sorption is calculated according to Equation (4).

$$\% \text{ sorption} = ((W_{60} - W_0)/W_0) \times 100 \quad (4)$$

where % sorption refers to the amount of water vapour absorbed by the fabric specimen during the test, and  $W_0$  and  $W_{60}$  are the specimen weights recorded before the start of the test and after 60 min.

In this study, tests were conducted on conditioned single-layer specimens as well as on double-layer assemblies (where a specimen was covered with a second fabric “cover layer” resembling that used in shoes). Two cover layers were used, namely, CP1, a knitted polyester that resembles the fabric in training shoes in terms of thickness and water vapour permeability, and CP2, a coated woven polyester with a low water vapour permeability, commonly used in shoes for leisure wear.



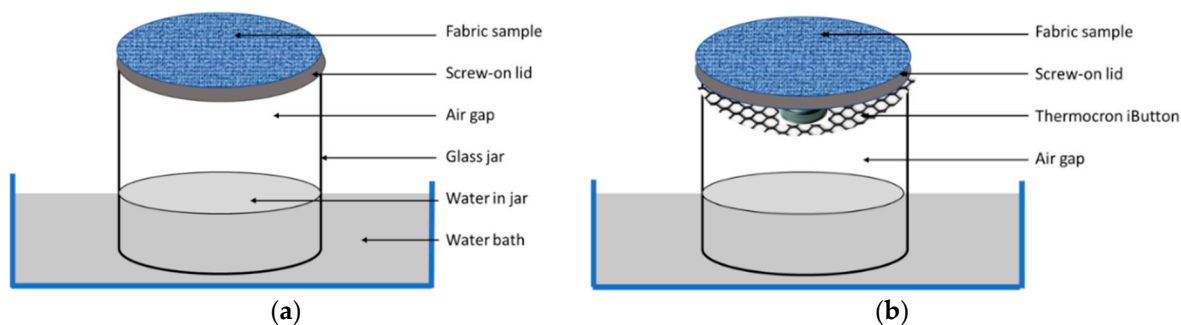


**Figure 7.** The laboratory setup of the CJ method, where (a) indicates the measurement of the % moisture sorption (part 1) and (b) the temperature and humidity inside the microclimate (part 2).

In the second part of the test, changes in humidity and temperature inside the jars were recorded with thermocron iButtons. To mount the iButtons inside the jar, a “scaffold” was created immediately below the sample using a nylon mesh fabric (Figure 7b). Care was taken to make sure that the button did not touch the sample surface or the water. Data were logged and recorded every 60 s for a total of 60 min.

### 3. Results and Discussion

Scanning electron microscope (SEM) images of the three yarns (MH, PETR, and BV) are depicted in Figure 8. In the MW yarn, the surface detail of the wool and mohair fibres can be seen, covered with sheet-like, hardened cuticle cells called scales. The scales overlap with exposed edges pointing towards the tip of the fibre. The scales on the mohair fibres are much less prominent and overlap less than those on wool fibres [2,28]. The image of yarn PETR depicts the typical smooth fibre surfaces of synthetic polyester fibres, and the BV yarn clearly shows the typical striated structure of viscose type yarns.



**Figure 8.** SEM images illustrating the physical structure of the fibres in the 3 main yarns used in this study. With (a) fibres in a yarn referenced as MW (mohair-wool), (b) yarn BV (bamboo viscose), and (c) yarn PETR (recycled polyester). The SEM magnification is 1000x and the images show a clear difference in the surface characteristics of the fibre types.

The thermal resistance ( $R_t$ ) and thickness of the specimens from the three socks were measured on the Alambeta instrument. Initial observations showed a variation in  $R_t$  and thickness among specimens cut from different parts of the same sock, even though all measurements on this instrument are taken under the same standard pressure to ensure consistency. The observed variations can be attributed to the industrial finishing process. In this process, socks are fitted over a standard foot frame and steam-finished to ensure consistent sizing, which can lead to stretching in certain areas and slight distortions in the

knit structure, resulting in thinner or thicker sections. These variations affect the amount of trapped still air within the fabric, consequently impacting its thermal resistance. It should also be kept in mind that socks are knitted structures containing elastane yarns, which are designed to fit snugly over a foot. During cutting, the specimens can, thus, relax and exhibit a slight change in dimensions, including thickness. For this reason, the initial statistical analyses of the results focused on the correlation between the  $R_t$  and fabric thickness. The Spearman rank-order test confirmed a positive correlation for the specimens containing MW ( $R = 0.89$ ,  $p < 0.01$ ) and BV ( $R = 0.72$ ,  $p < 0.01$ ). In the case of PETR, the effect was not significant ( $p > 0.01$ ). The scatterplots in Figure 9 depict the correlation between thermal resistance and fabric thickness per individual fabric (MW, PETR, and BV), confirming the Spearman rank-order tests.

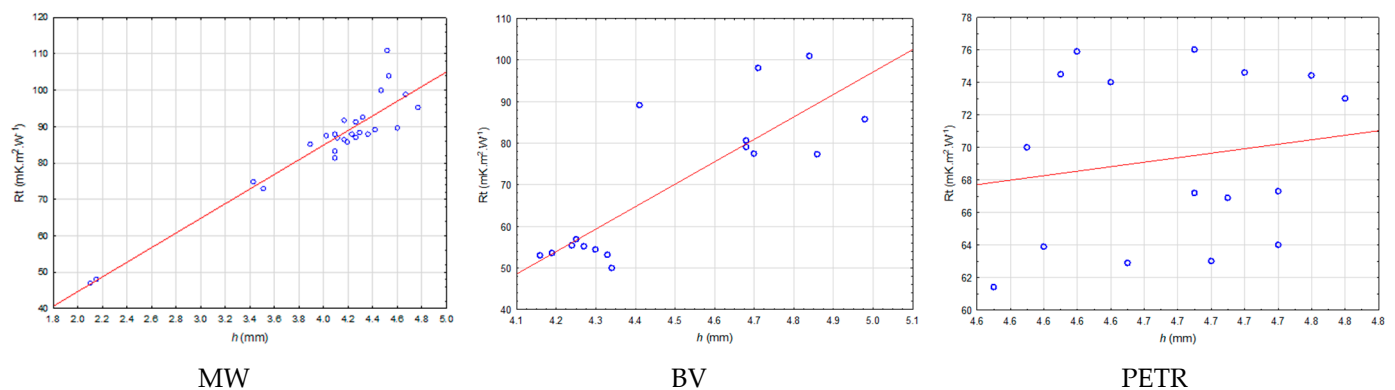


**Figure 9.** Scatterplots depicting the thermal resistance ( $R_t$ ) versus thickness ( $h$ ) of fabrics tested on the Alambeta.

The effect of the range of fabric weights that were measured after samples were cut from the socks is clear in Figure 9. Resultantly, for a better interpretation of the effect of fibre content on the  $R_t$  results, the median thickness of the fabric samples was determined ( $4.42 \text{ mm}$ ) and only specimens within a comparable thickness range ( $4.42 \pm 5\%$ ) were selected for the statistical evaluation. An analysis of variance (ANOVA) was conducted to determine the influence of fibre content on  $R_t$  values, while controlling the fabric thickness. The analysis focused on data where thickness fell within a predefined range. Figure 10 depicts the ANOVA results, clearly indicating a statistically significant difference in  $R_t$  between the MW, BV, and PETR fabrics. The MW fabric exhibited the highest  $R_t$ , while the BV fabric displayed the lowest  $R_t$ . This is in accordance with the known thermal conductivity of wool, polyester, and viscose fibres [2,29].

To assess thermal resistance under conditions mimicking actual wear (unlike measurements on isolated fabric samples), the  $R_t$  of the complete socks was evaluated using the TFM. The average measurement per sock over the 13 segments was calculated and the analysis of variance in the results are shown in Figure 11. Measurements of the complete sock's  $R_t$  on the thermal foot diverged from the values obtained for individual fabric specimens (as shown in Figure 10). The most important observation was that the sock  $R_t$  (TFM) and sock thickness were highly dependent on each other. The Spearman rank-order test indicated a highly positive correlation ( $R = 0.766$ ,  $p < 0.05$ ), which confirms that the sock thickness was the most important factor determining the ability of the socks to conduct or retain heat. This is illustrated in the scatterplot in Figure 11 below.

A comparison of the three sock samples to assess the effect of fibre content was performed statistically and the results can be seen in Figure 12. The thermal resistance of the socks containing MW and PETR did not differ significantly, but that of the S-MWV sock (that contained panels of MW and bamboo viscose) was significantly lower. The analysis confirms that the intentional design of the S-MWV sock to cause an overall cooling effect through strategically placed BV areas proved to be successful. (The difference in  $R_t$  between the MW and BV fibres is confirmed in Figure 10). The comparison of  $R_t$  results between the

Alambeta data (cut specimens) and TFM data (complete socks) highlights the limitation of relying on a single method to assess a complex parameter such as  $R_t$  in a garment.

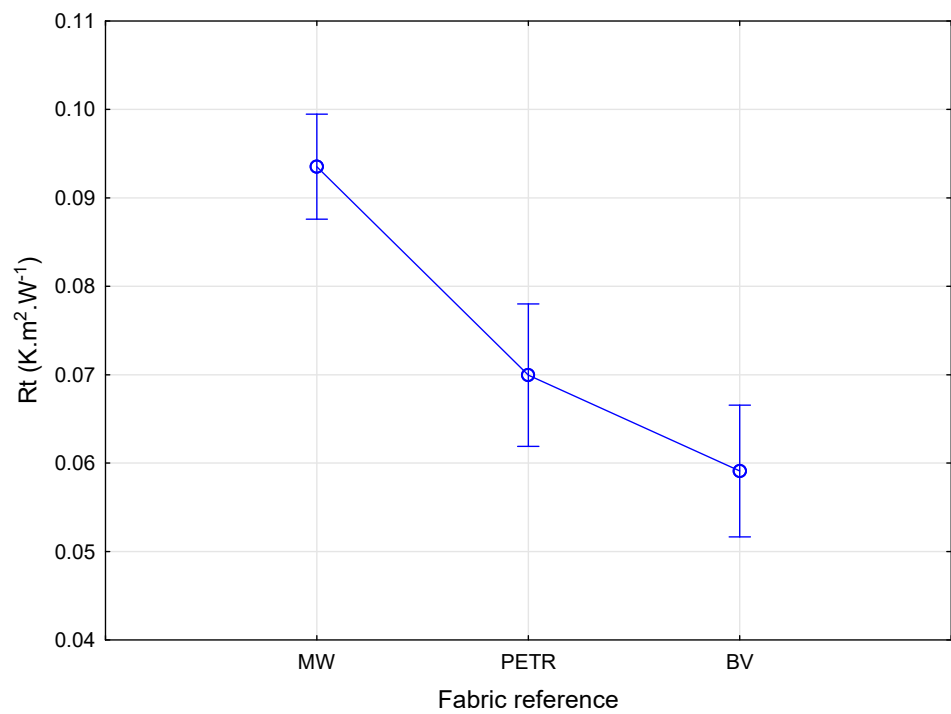


**Figure 10.** Effect of fibre content on thermal resistance ( $R_t$ ) as measured on the Alambeta. Vertical bars denote the 95% confidence intervals.

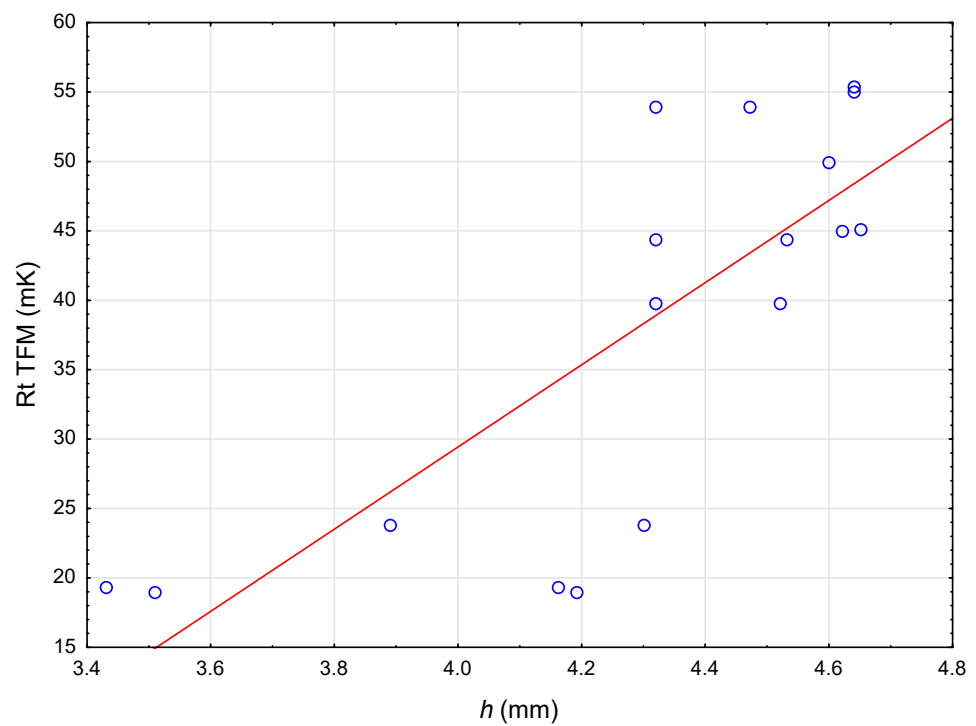


**Figure 11.** Scatterplot depicting the highly positive correlation between fabric thickness ( $h$ ) and thermal resistance ( $R_t$ ) measured on the thermal foot manikin (TFM).

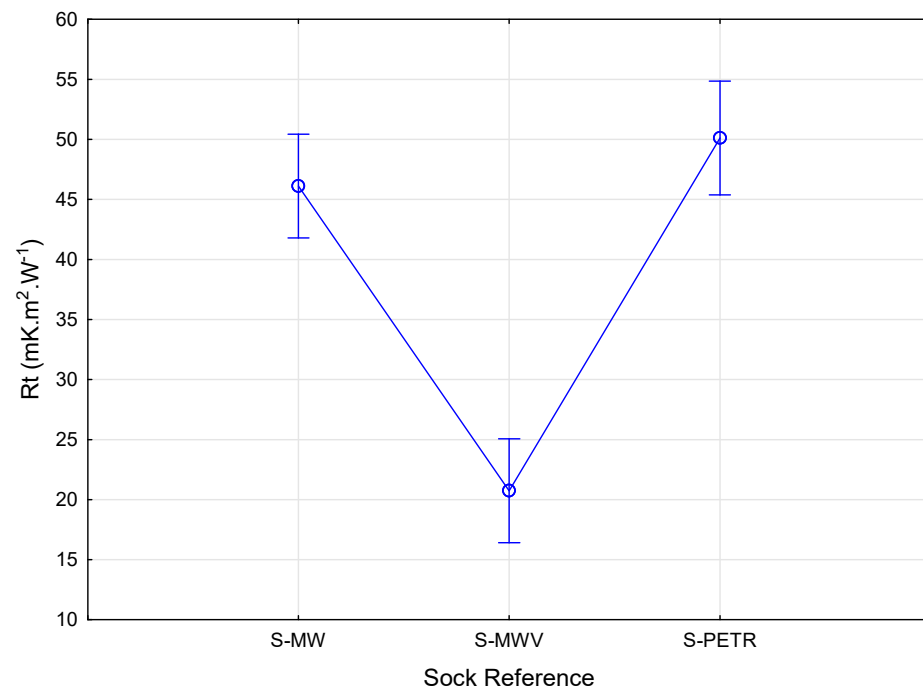


**Figure 12.** ANOVA of thermal resistance ( $R_t$ ) of socks as measured on TFM, indicating the differences between the three sock samples. Vertical bars denote the 95% confidence intervals.

The effects of variations in fabric thickness, as well as sock design, regarding fibre content on the thermal resistance ( $R_t$ ) of the sock (as measured on the TFM) are illustrated in the 3D scatterplot of thermal resistance ( $R_t$ ) plotted against fabric thickness ( $h$ ) and sock reference in Figure 13.

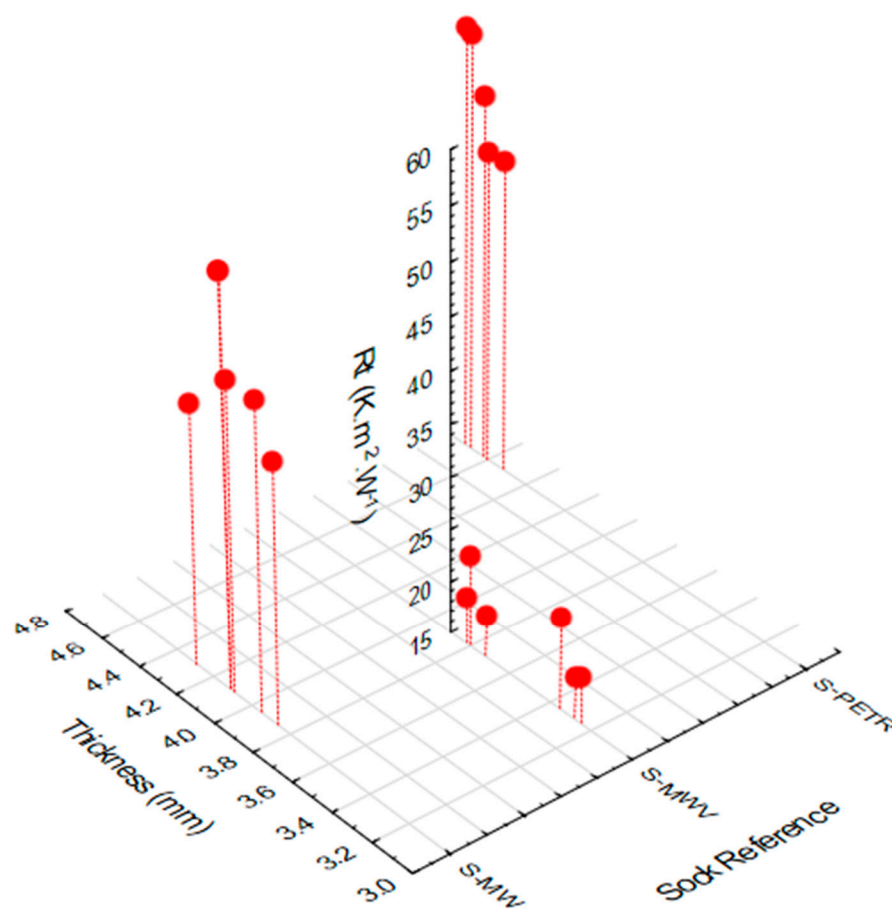
To gain a more comprehensive understanding of the thermo-physiological comfort provided by the sock samples, subsequent testing prioritised methods that assessed both thermal and moisture management within the microclimate. During wear trials the temperature and humidity levels in the microclimate inside the socks were logged over 60 min with iButtons positioned between the skin and the sock during wear. The measured data are illustrated in the graphs in Figure 14. The average values for temperature and humidity for TS1 and TS2 are summarised in Table 4.

Figure 14a depicts the temperatures measured over two time segments, namely, TS1 (from 1 to 40 min) and TS2 (from 40 to 60 min). The trends observed in the microclimate temperatures in both TS1 and TS2 reflect the  $R_t$  measurements on the TFM. (It should be noted that the iButton measurements reflect the actual temperatures measured, whereas the TFM measures the thermal resistance ( $R_t$ ) of the socks.) The temperatures measured when the S-MWV sock was worn were consistently lower than those measured inside the other two samples, especially in the TS2 (more active) time segment, confirming the TFM results.

While a trend emerged (MW values trending slightly lower than PETR later in the cycle), humidity proved challenging to measure accurately due to the limited microclimate within a sock, especially in TS2 when the possibility of sweat production was increased. It should be noted that if the iButton comes into contact with any liquid water during the test, it has an immediate effect on the measurement, as can be seen in the spikes in the graph.

**Table 4.** Summary of results of Rt (Alambeta), Rt (TFM), Microclimate temperature and humidity (wear trials and CJ method) and moisture sorption (CJ method).

Sock Ref.	Fabric Ref.	Rt (Alambeta)	Rt (TFM)	Temperature		Humidity		Temperature (Microclimate in CJ)	Humidity (Microclimate in CJ)	Moisture Sorption (CJ Method)
				(Microclimate in Wear Trial)		(Microclimate in Wear Trial)				
				TS1	TS2	TS1	TS2			
		$\text{mK}\cdot\text{m}^2\cdot\text{W}^{-1}$	$\text{mK}\cdot\text{m}^2\cdot\text{W}^{-1}$	$^{\circ}\text{C}$	$^{\circ}\text{C}$	%	%			%
S-MW	MW	93.5	46.1	33.5	34.3	51.4	52.9	26.4	69	2.20
S-PETR	PETR	70.0	50.2	32.9	34.2	51.4	52.3	26.8	72.7	0.53
S-MWV	BV	59.1	27.4	31.6	33.1	49.3	50.3			
	MW + CP1							27.5	71.7	1.70
	MW + CP2							29.4	75.4	7.38
	PETR + CP1							27.8	81.5	0.55
	PETR + CP2							29.2	87.1	2.87



**Figure 13.** Scatterplot of fabric thickness ( $h$ ) and thermal resistance ( $R_t$ ) (measured on TFM) plotted against sock reference.

Building on the insights from the wear trials, the CJ test method was developed to address the limitations encountered during that stage. Only PETR and MW samples (cut from sock samples S-MW and S-PETR) were tested, as these are the fibre compositions of the areas surrounding the foot in the critical areas where the requirements for diabetic socks need to be met. The results are shown in Table 4. The CJ method corroborated and provided a clearer picture of the wear performance differences between S-MW and S-PETR socks observed in the wear trial results. For the uncovered (single-layer) fabrics, the initial temperature as well as humidity in the microclimate in the jar (under the PETR specimens) increased more than in the case of the MW specimens. It stabilised after about 13 min and remained higher for the rest of the test period. Where the test specimens were covered with CP1, the same trend was noticed regarding the temperature in the microclimate, but the difference between MW and PETR was higher. The humidity levels did not change significantly. When the denser CP2 fabric was used to cover the MW and PETR, the temperature graphs changed. The PETR showed an immediate increase to above 30 °C, but the general increase in the case of the MW specimens was higher. The values became similar as it stabilised but remained much higher than for the more permeable cover CP1 and uncovered samples. The  $R_t$  measurements from both the Alambeta and TFM instruments are corroborated by these findings. Notably, the higher  $R_t$  of the MW fabric becomes more pronounced as the permeability of the cover fabric decreases. These results are visualised in the graph of Figure 15a. The average temperatures measured in the CJ tests are lower than those measured during the wear trials. This can be attributed to the differences in the size of the respective microclimates. Further development of the CJ test should focus on decreasing the air gap in the jar between the water and the specimen.

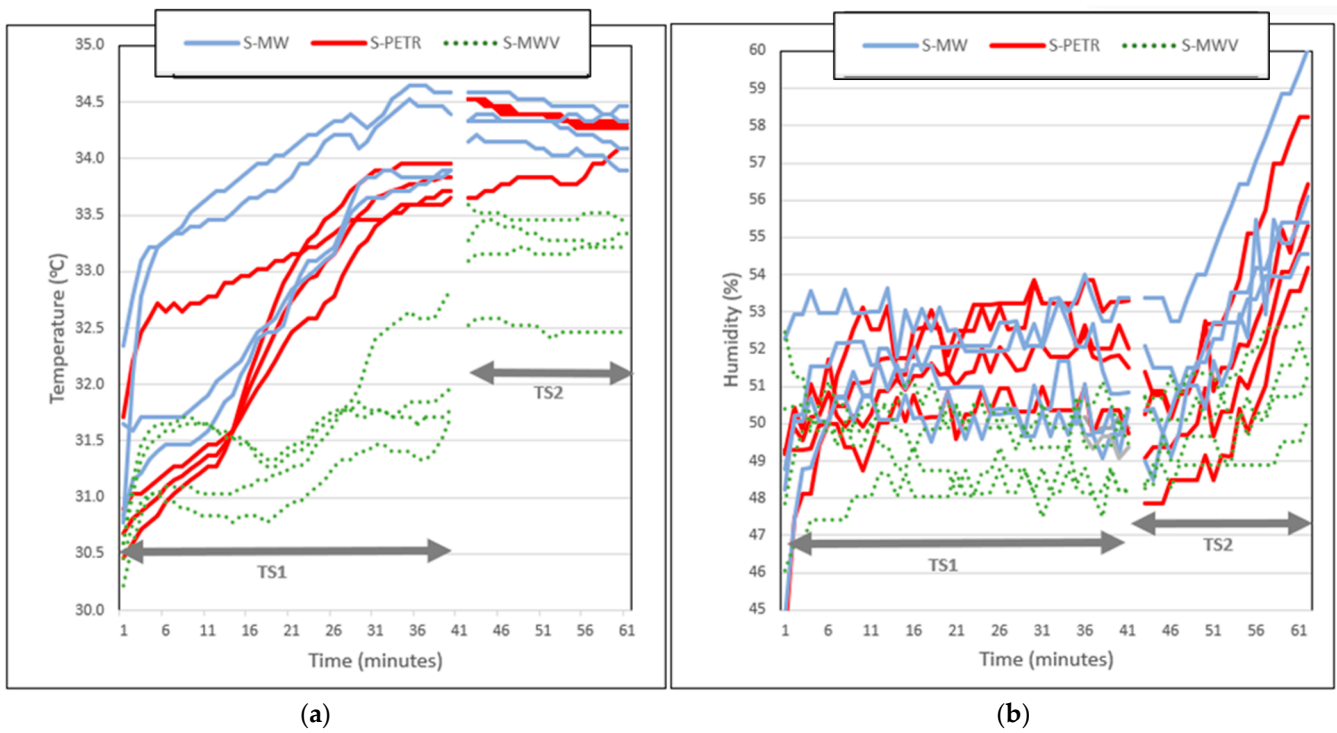


**Figure 14.** The temperature (a) and humidity (b) measurements in the microclimate logged with thermochron iButtons during wear trials during which the S-PETR, S-MW, and S-MWV socks were worn.

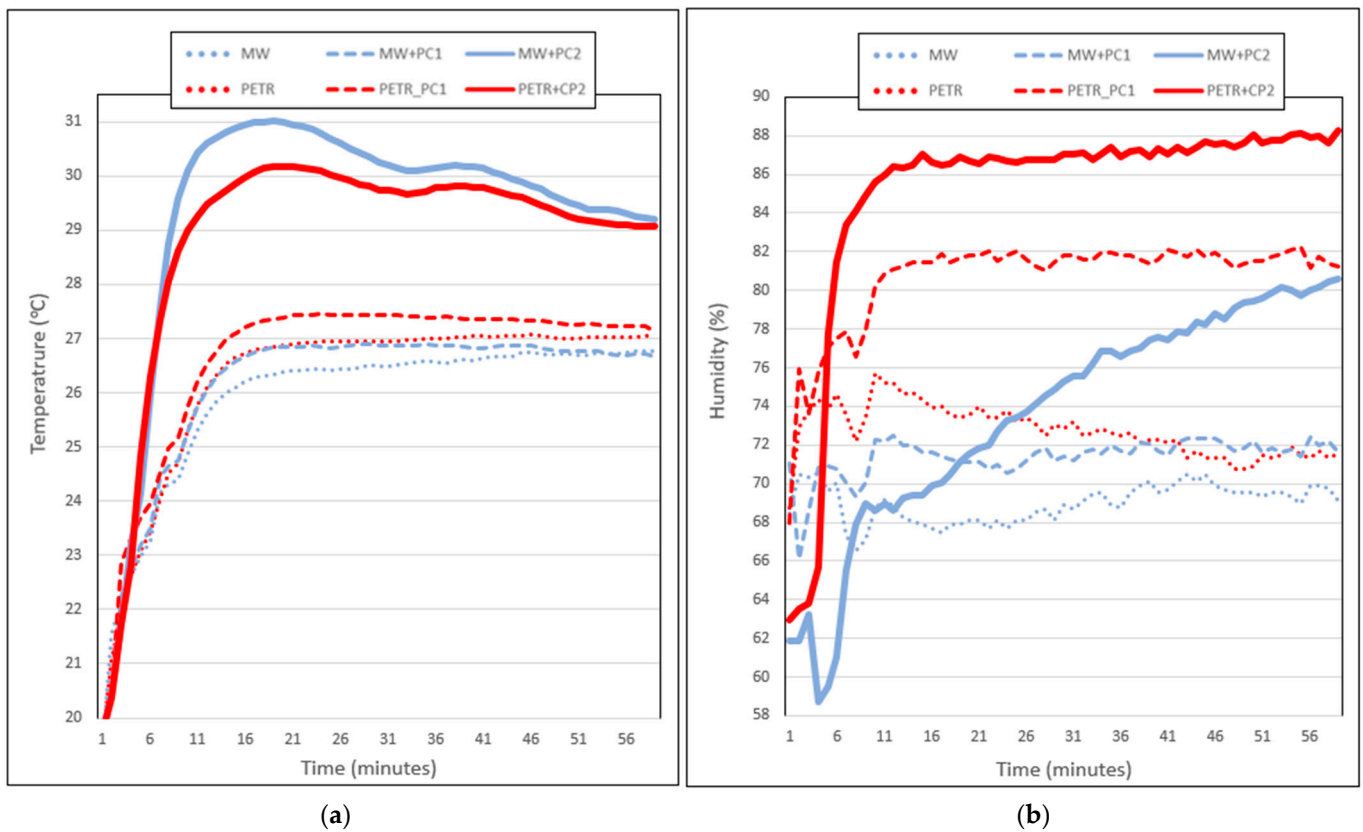


**Figure 15.** The temperature (a) and humidity (b) measurements in the microclimate logged over 60 min with thermochron iButtons during the CJ method (part 2) tests on the PETR and MW fabrics.

The humidity levels depicted in Figure 15b explain the differences in the moisture management properties of the MW and PETR fabrics. In the case of the uncovered specimens, and where the specimens were covered by the highly moisture vapour permeable CP1 cover, moisture vapour is allowed to escape to the environment and build-up in the microclimate is limited. The hygroscopic MW fibres performed better than the synthetic PETR fibres. The average humidity inside the microclimate for the single-layer, sample + CP1, and sample + CP2 evaluations were, respectively, 69%, 71.7%, and 75.4% for MW and 72.7%, 81.5%, and 87.5% for PETR (Table 4 and Figure 16). When the CP2 layer (that has a very low moisture vapour permeability) was added, the humidity inside the microclimate increased significantly. This is more pronounced in the case of the PETR fabric. As explained in the literature, the hygroscopic properties of the MW, which allows the sorption of moisture vapour without wetting the fabric, causes the conditions in the microclimate to change slower over time. As the fabric became more saturated, the humidity increased, but not to the same extent as with the PETR. In part 1 of the CJ method, the % moisture sorption in the specimens (after 60 min of exposure to permeating water vapour) was determined. The analysis of variance (ANOVA) in Figure 16 reveals a statistically significant difference in the amount of moisture absorbed by the MW specimens compared to the others. This difference is likely due to the unique properties of the MW fibres. We propose that the MW fibres possess a greater capacity to absorb and retain moisture within their structure. This is particularly evident when the CP2 cover restricts the diffusion of water vapour. By absorbing the moisture, the MW fibres prevent its accumulation within the micro-climate, but allow for the postulated self-regulating mechanism to occur. In contrast, the PETR fibres exhibited minimal moisture sorption. This resulted in a higher relative humidity within the microclimate due to the presence of unabsorbed water vapour.

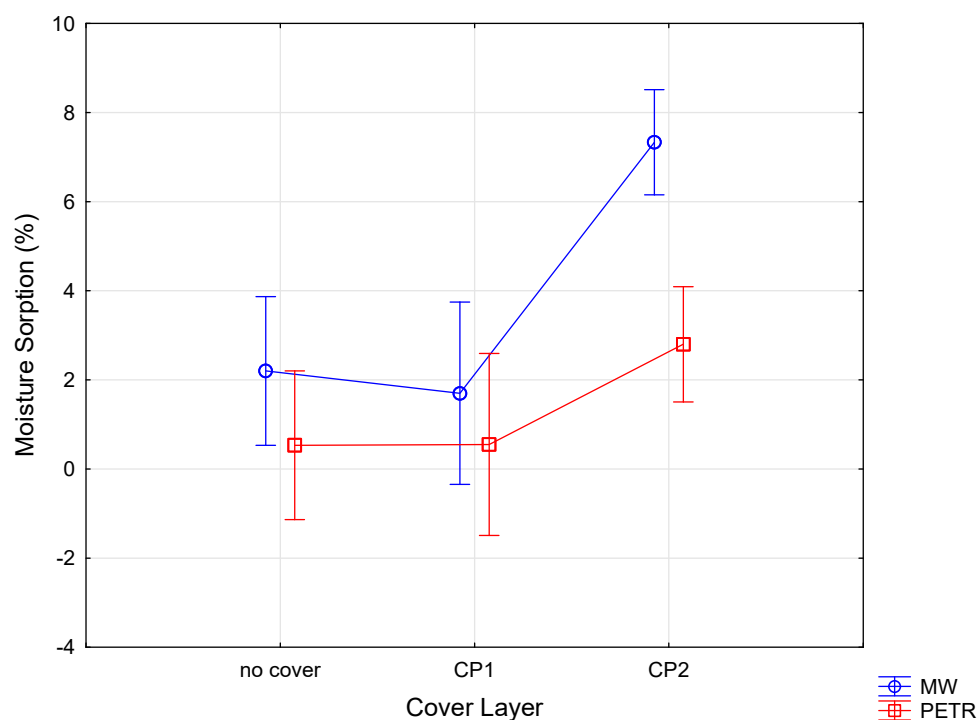


**Figure 16.** Analysis of variance depicting the % sorption measured during the CJ method (part 1) tests on the PETR and MW fabrics, with no cover and covered with CP1 and CP2.

#### 4. Conclusions

This study investigated the thermal and moisture management properties of knitted socks for diabetic patients. Regarding thermal resistance, fabric structure, especially fabric thickness, had a greater impact on thermal resistance than fibre composition. This implies that the design of the socks can allow for customisation based on individual needs to cater



to preferences for cooler or warmer socks. The results also emphasise the need to not rely on one test method when testing a complex performance property such as the thermal resistance of a product.

Additionally, mohair–wool socks outperformed polyester socks in terms of moisture management. Wear trials and the novel microclimate test method revealed significantly lower humidity within the mohair–wool sock compared to the polyester sock, regardless of which cover was used to simulate the shoe cover. This aligns with the mohair–wool fabric’s superior moisture vapour sorption, exceeding that of polyester by a significant margin. These findings demonstrate that mohair–wool socks can help maintain a healthy microclimate around the skin and may be a good choice for diabetic patients where optimum foot care is a priority.

The novel test method that was developed to measure the change in the conditions in the microclimate, as well as the % moisture sorption in the fabric specimens over time, provided valuable insight in the performance of the tested socks and can be regarded as a significant contribution to further research in this field.

**Author Contributions:** Conceptualization, A.G.; methodology, A.G.; software, A.G.; validation, A.G. and M.V.; formal analysis, A.G.; investigation A.G.; resources A.G. and M.V.; data curation, A.G.; writing—original draft preparation, A.G.; writing—review and editing, M.V.; visualization, A.G. and M.V.; supervision, M.V.; project administration, M.V.; funding acquisition, M.V. All authors have read and agreed to the published version of the manuscript.

**Funding:** This work was supported by the Czech Science Foundation (GACR)—project Advanced Structures for thermal insulation in extreme conditions (Reg. No. 21-32510M).

**Data Availability Statement:** The data supporting the conclusions of this article is contained within the article.

**Conflicts of Interest:** The authors declare no conflict of interest.

## References

- Botha, A.F.; Hunter, L. *A Comparative Study of the Healthcare and Wellness Related Properties of Mohair*; African Sun Media: Port Elizabeth, South Africa, 2013.
- Gericke, A.; Militky, J.; Venkataraman, M.; Steyn, H.J.; Vermaas, J. Investigation of Thermal Comfort Properties of Fabrics Containing Mohair. *J. Text. Inst.* **2022**, *113*, 616–627. [[CrossRef](#)]
- Wu, S.C.; Driver, V.R.; Wrobel, J.S.; Armstrong, D.G. Foot Ulcers in the Diabetic Patient, Prevention and Treatment. *Vasc. Health Risk Manag.* **2007**, *3*, 65–76.
- Iraj, B.; Khorvash, F.; Ebneshahidi, A.; Askari, G. Prevention of Diabetic Foot Ulcer. *Int. J. Prev. Med.* **2013**, *4*, 373–376. [[PubMed](#)]
- Elsayed, E.M.; Elsaman, S.I.L. Synthesis of Smart Medical Socks for Diabetic Foot Ulcers Patients. *Fibers Polym.* **2017**, *18*, 811–815. [[CrossRef](#)]
- Borkow, G.; Zatcoff, R.C.; Gabbay, J. Reducing the Risk of Skin Pathologies in Diabetics by Using Copper Impregnated Socks. *Med. Hypotheses* **2009**, *73*, 883–886. [[CrossRef](#)]
- Rogina-Car, B.; Skenderi, Z.; Vrljičak, Z. Thermal Resistance of Viscose Socks. *Koža Obuća* **2019**, *68*, 18–21. [[CrossRef](#)]
- Rogina-Car, B.; Skenderi, Z.; Vrljičak, Z. Thermophysiological Wear Comfort of Viscose and Tencel Socks. *Koža Obuća* **2020**, *68*, 22–29. [[CrossRef](#)]
- Das, B.; Das, A.; Kothari, V.K.; Fanguiero, R.; de Araújo, M. Moisture Transmission through Textiles: Part I: Processes Involved in Moisture Transmission and the Factors at Play. *Autex Res. J.* **2007**, *7*, 100–110. [[CrossRef](#)]
- Bhatia, D.; Malhotra, U. Thermophysiological Wear Comfort of Clothing: An Overview. *J. Text. Sci. Eng.* **2016**, *6*, 1–8. [[CrossRef](#)]
- Hatch, K.I. *Textile Science*; West Group: Eagen, MN, USA, 1993; ISBN 13: 9780314904713.
- Kadolph, S.; Marcketti, S. *Textiles*, 12th ed.; Pearson Education, US: Upper Saddle River, NJ, USA, 2016; ISBN 9780131187696.
- Afzal, A.; Ahmad, S.; Rasheed, A.; Ahmad, F.; Iftikhar, F.; Nawab, Y. Influence of Fabric Parameters on Thermal Comfort Performance of Double Layer Knitted Interlock Fabrics. *Autex Res. J.* **2017**, *17*, 20–26. [[CrossRef](#)]
- Kaplan, S.; Karaman, C. Thermal Comfort Performances of Cellulosic Socks Evaluated by a Foot Manikin System and Moisture Management Tester. *Int. J. Cloth. Sci. Technol.* **2019**, *1*, 272–283. [[CrossRef](#)]
- Majumdar, A.; Mukhopadhyay, S.; Yadav, R. Thermal Properties of Knitted Fabrics Made from Cotton and Regenerated Bamboo Cellulosic Fibres. *Int. J. Therm. Sci.* **2010**, *49*, 2042–2048. [[CrossRef](#)]
- Holcombe, B.V.; Hoschke, B.N. Part IV: Prediction of Tensile Properties. *Text. Res. J.* **1983**, *53*, 368–374. [[CrossRef](#)]
- Militký, J.; Křemenáková, D. Simple Methods for Prediction of Textile Fabrics Thermal. In Proceedings of the 5th International Conference on Heat Transfer, Fluid Mechanics and Thermodynamics, Sun City, South Africa, 1–4 July 2007.

18. Marolleau, A.; Salaun, F.; Dupont, D.; Gidik, H.; Ducept, S. Influence of Textile Properties on Thermal Comfort. *IOP Conf. Ser. Mater. Sci. Eng.* **2017**, *254*, 182007. [[CrossRef](#)]
19. Hes, L.; Dolezal, I. New Method Thermal and Equipment for Measuring Properties of Textiles. *Sen'i Kikai Gakkaishi (J. Text. Mach. Soc. Japan)* **1989**, *42*, 71–75.
20. Hes, L. Laboratory Measurement of Thermo-Physiological Comfort. In *Improving Comfort in Clothing*; Song, G., Ed.; Woodhead Publishing Ltd.: Cambridge, UK, 2011; pp. 114–137.
21. Özgen, B.; Altaş, S. The Investigation of Thermal Comfort, Moisture Management and Handle Properties of Knitted Fabrics Made of Various Fibres. *Tekst. Ve Konfeksiyon* **2014**, *24*, 266–271.
22. Karthikeyan, G.; Nalankilli, G.; Shanmugasundaram, O.L.; Prakash, C. Thermal Comfort Properties of Bamboo Tencel Knitted Fabrics. *Int. J. Cloth. Sci. Technol.* **2016**, *28*, 420–428. [[CrossRef](#)]
23. Hes, L.; Dolezal, I. Indirect Measurement of Moisture Absorptivity of Functional Textile Fabrics. *J. Phys. Conf. Ser.* **2018**, *1065*, 122026. [[CrossRef](#)]
24. Hes, L. Non-Destructive Determination of Comfort Parameters during Marketing of Functional Garments and Clothing. *Indian J. Fibre Text. Res.* **2008**, *33*, 239–245.
25. Yılma, B.B.; Luebben, J.F.; Tadesse, M.G. Effect of Plasma Surface Modification on Comfort Properties of Polyester/Cotton Blend Fabric. *Mater. Res.* **2021**, *24*, e20210021. [[CrossRef](#)]
26. Mansoor, T.; Hes, L.; Bajzik, V.; Noman, M.T. Novel Method on Thermal Resistance Prediction and Thermo-Physiological Comfort of Socks in a Wet State. *Text. Res. J.* **2020**, *90*, 1987–2006. [[CrossRef](#)]
27. Gericke, A.; Militký, J.; Venkataraman, M.; Steyn, H.; Vermaas, J. The Effect of Mask Style and Fabric Selection on the Comfort Properties of Fabric Masks. *Materials* **2022**, *15*, 2559. [[CrossRef](#)] [[PubMed](#)]
28. Hunter, L. *Mohair: A Review of Its Properties, Processing and Applications*; CSIR Division of Textile Technology: Port Elizabeth, South Africa, 1993; ISBN 798837179.
29. Militký, J.; Křemenáková, D. Thermal Conductivity of Wool/Pet Weaves. *HEFAT* **2008**. Available online: <http://hdl.handle.net/2263/42905> (accessed on 12 June 2024).

**Disclaimer/Publisher's Note:** The statements, opinions and data contained in all publications are solely those of the individual author(s) and contributor(s) and not of MDPI and/or the editor(s). MDPI and/or the editor(s) disclaim responsibility for any injury to people or property resulting from any ideas, methods, instructions or products referred to in the content.